

Advection-enhanced diffusion in biased convection arrays

Yunyun Li¹, Qingqing Yin¹, Fabio Marchesoni^{1,2,*}, Tanwi Debnath³, and Pulak K. Ghosh^{4,†}¹Center for Phononics and Thermal Energy Science, Shanghai Key Laboratory of Special Artificial Microstructure Materials and Technology, School of Physics Science and Engineering, Tongji University, Shanghai 200092, China²Dipartimento di Fisica, Università di Camerino, I-62032 Camerino, Italy³Department of Chemistry, University of Calcutta, Kolkata 700009, India⁴Department of Chemistry, Presidency University, Kolkata 700073, India

(Received 13 December 2020; accepted 11 March 2021; published 29 March 2021)

We numerically investigated the transport of a passive colloidal particle in a one-dimensional periodic array of planar counter-rotating convection rolls at high Péclet numbers. We show that advection-enhanced diffusion is drastically suppressed by an external transverse bias but strongly reinforced by a longitudinal drive of appropriate intensity. Both effects are magnified by imposing free-slip flows at the array's edges. The dependence of the diffusion constant on an external forcing is interpreted as a measure of the fluid-mechanical robustness of the flow boundary layer mechanism governing diffusion in convection rolls.

DOI: [10.1103/PhysRevE.103.L030106](https://doi.org/10.1103/PhysRevE.103.L030106)

Introduction. Diffusion of a passive Brownian particle advectioned by a laminar flow is a recurrent problem in today's nanotechnology [1–3]. One encounters this problem at the most diverse spatial scales, from the design of microfluidic chips [1,3], to the kinematic dynamo models in plasma physics [4,5]. In particular, the phenomenon of advection enhanced diffusion (AED) is key to understanding mass and heat transport in geophysical processes and has applications in chemical engineering and combustion [6].

As a study case of diffusion in a laminar convective flow, we considered an overdamped pointlike Brownian particle of unit mass suspended in an array of counter-rotating convection rolls of stream function [7,8]

$$\psi(x, y) = (U_0 L / 2\pi) \sin(2\pi x / L) \sin(2\pi y / L). \quad (1)$$

Here, L is the size of the flow unit cell, U_0 the maximum advection speed at the roll separatrices, $\Omega_L = 2\pi U_0 / L$ the maximum vorticity at their centers, and $D_L = U_0 L / 2\pi$ an intrinsic flow diffusion constant. The orthogonal coordinate, z , is ignorable, so that we deal with an effectively two-dimensional (2D) problem. When subjected to thermal fluctuations of strength D_0 , the particle undergoes normal diffusion with asymptotic diffusion constant D . At high Péclet numbers, $Pe = D_L / D_0 \gg 1$, the constant D is appreciably larger than the free diffusion constant, D_0 . This AED manifestation has been explained [7–10] by noticing that, at low noise, an unbiased particle jumps between convection rolls while being advected along the roll outer flow layers. Such flow boundary layers (FBLs) form a network of advection channels of estimated width $\delta = (D_0 / \Omega_L)^{1/2}$, centered around the rolls' separatrices, which thus favors the particle's spatial diffusion. By contrast, roll jumping due to thermal fluctuations is way

less effective, even if the stationary particle's probability density function (pdf) inside the $\psi(x, y)$ unit cells is uniform [11].

AED has been reported for both square [7,8] and linear arrays [9,10] of convection rolls. The underlying FBL mechanism, however, fails for non-center-symmetric stream functions [12]. There the stream function separatrices split and narrow easy-flow channels open up between parallel one-dimensional (1D) arrays of convection rolls. As the width of such channels grows of the order of δ , AED is deactivated.

In this Letter we investigate distinct and possibly more general manifestations of tunable AED, i.e., advection in the presence of a bias. We observed that AED in a 1D array of convection rolls [convection array for short, Fig. 1(a)] becomes sharply suppressed upon raising the intensity of an applied transverse force. This result suggests that the external force blocks the particle's circulation in the FBL's, thus causing their sudden breakup. By contrast, in the presence of a longitudinal force, the FBL branches parallel to the array edges keep governing particle's diffusion. This is signaled by a huge excess-diffusion peak for values of the force intensity of the order of the advection drag, U_0 . Both effects occur independently of the slip properties of the flow at the array edges, though more appreciably in free-boundary arrays.

Model. A Brownian particle of coordinates x and y , diffusing in the convection array of stream function $\psi(x, y)$, Eq. (1) with $0 \leq y \leq L/2$, obeys the Langevin equations (LE),

$$\dot{x} = u_x + F_x + \xi_x(t), \quad \dot{y} = u_y + F_y + \xi_y(t), \quad (2)$$

where $\mathbf{u} = (u_x, u_y) = (\partial_y, -\partial_x)\psi$ is the incompressible advection velocity vector, $\nabla \cdot \mathbf{u} = 0$, and $\mathbf{F} = (F_x, F_y)$ denotes a tunable, uniform force applied to the array. As illustrated in Fig. 1(a), the array unit cell consists of two counter-rotating convection rolls. Reflecting boundaries are assumed for the particle's trajectories at the array edges, $y = 0$ and $L/2$. The random sources, $\xi_i(t)$ with $i = x, y$, are stationary, independent, delta-correlated Gaussian noises, $\langle \xi_i(t) \xi_j(0) \rangle = 2D_0 \delta_{ij} \delta(t)$, modeling equilibrium thermal fluctuations in a

*fabio.marchesoni@pg.infn.it

†pulak.chem@presiuniv.ac.in

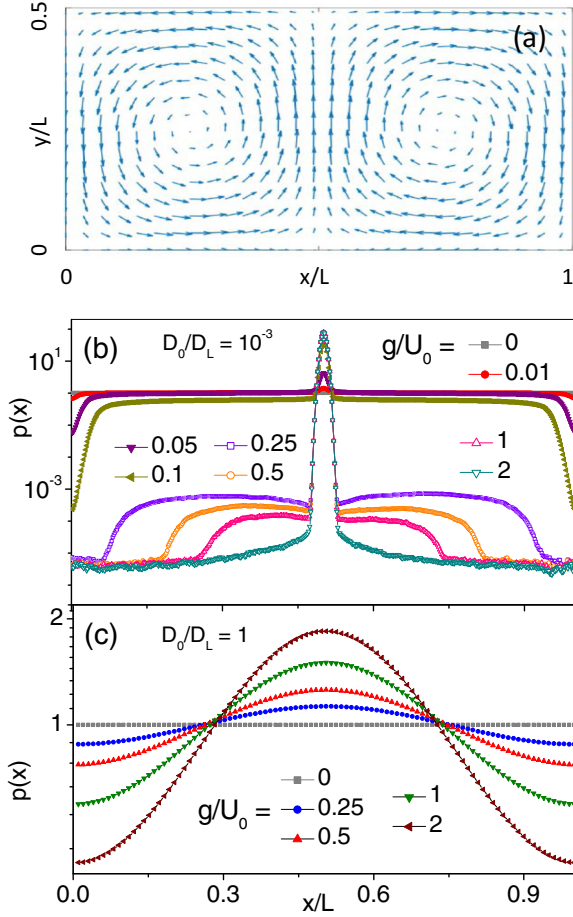


FIG. 1. Diffusion of a Brownian particle in a convection array with stream function of Eq. (1) and $0 \leq y \leq L/2$. (a) Array's unit cell. Boundary conditions are reflecting for $y = 0, L/2$, and periodic for $x = 0, L$. (b) Longitudinal probability density functions (pdfs) for different D_0 and g (see legends). pdfs obtained by distributing the particle's x coordinate according to a one-cell representation. The flow parameters are $U_0 = 1$ and $L = 2\pi$, hence $D_L = 1$.

homogeneous, isotropic medium. In our notation, D_0 coincides with the free-particle diffusion constant in the absence of advection. The flow parameters, L and U_0 , define convenient length and time units, respectively, L and Ω_L^{-1} . Therefore the only tunable parameters left in our analysis are the noise strength, D_0 (in units of D_L), and the bias components, F_x, F_y (in units of U_0). The stochastic differential equations, Eqs. (2), were numerically integrated by means of a standard Mil'shtein scheme [13]. To ensure numerical stability, the numerical integrations have been performed using a very short time step, 10^{-5} – 10^{-4} . The particle's spatial distributions, shown in Figs. 1(b) and 1(c), have been computed over at least 10^7 samples (trajectories). Computing the asymptotic diffusion constant [14], $D = \lim_{t \rightarrow \infty} \langle \Delta x^2(t) \rangle / 2t$, with $\Delta x(t) = x(t) - \langle x(t) \rangle$, required extra caution, because for $Pe \gg 1$, the advected particle may take an exceedingly long time to exit a convection roll.

As illustrated in Fig. 2, at zero bias the asymptotic diffusion constant D changes from $D = \kappa \sqrt{D_L D_0}$ for $Pe \gg 1$ (advective diffusion) to $D = D_0$ for $Pe \ll 1$ (thermal dif-

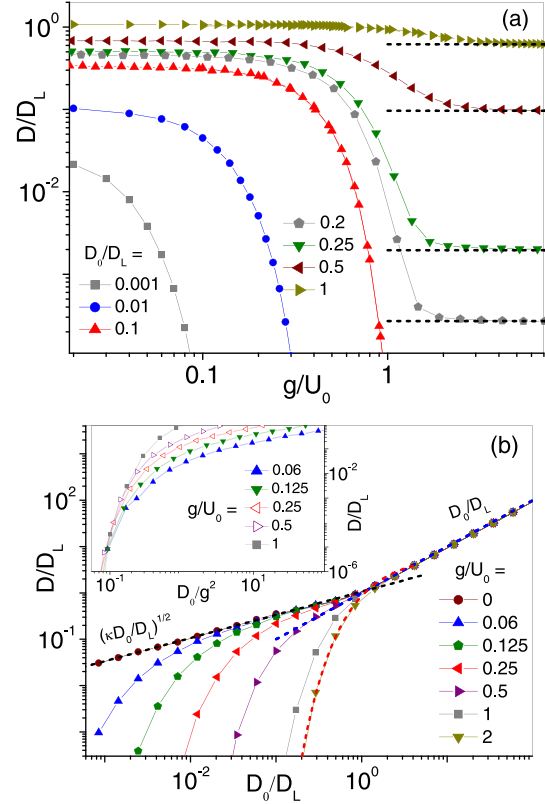


FIG. 2. Diffusion in a convection array of Eq. (1) with transverse bias. Asymptotic diffusion constant, D/D_L , vs (a) g/U_0 for different D_0 , and (b) D_0/D_L for different g . Inset: rescaled curves from panel (b) to illustrate the FBL breakup mechanism. The analytical estimate of D , Eq. (4) with $\langle \cos(2\pi y/L) \rangle = 1$, is represented by dashed lines in (a), and a dashed curve in (b). The flow parameters are $U_0 = 1$ and $L = 2\pi$, with $D_L = 1$.

fusion). The constant κ depends on the convection array's geometry and boundary conditions [7,10]. For the unbiased, free-boundary convection array of Eq. (1), $\kappa \simeq 1.065$ [7], consistently with the numerical results of Fig. 2(b). The crossover between these two diffusion regimes is well localized at around $D_0 \simeq D_L$ [15]; accordingly, AED sets in for $Pe > 1$. Indeed, as anticipated in the Introduction, numerical evidence [15] demonstrates that for $Pe \gg 1$ spatial diffusion takes place mostly along the FBL's delimiting the convection rolls [7,8,10]. Vice versa, for $Pe \ll 1$ the effects of advection are superseded by translational thermal fluctuations. Many numerical and experimental studies support this interpretation of AED [16–20].

Transverse bias. The most prominent effect of a transverse bias, say, $\mathbf{F} = (0, -g)$, is the drastic drop of the particle's diffusion constant, D , for $Pe \gg 1$, Fig. 2. Note that the data in panel (a) are restricted to $Pe \geq 1$, whereas the data in panel (b) span over both Péclet regimes. The drop of D upon increasing g , panel (a), or decreasing D_0 , panel (b), is very sharp. Also remarkable is that AED gets suppressed for bias values which appear to increase with D_0 [inset of Fig. 2(b)]. In parallel with this dynamical transition, the profile of the particle's longitudinal distribution undergoes an abrupt change. The pdfs of Fig. 1(b), $p(x)$, grow from uniform, as to be

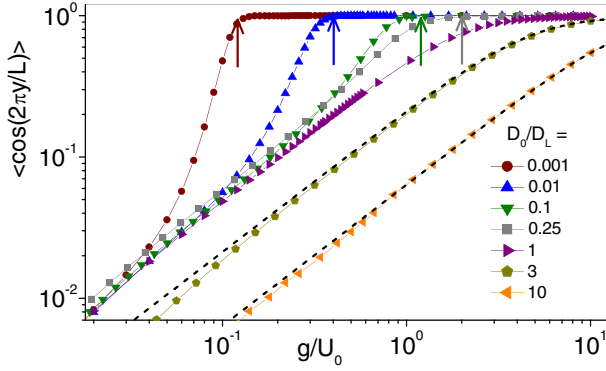


FIG. 3. Diffusion in a convection array of Eq. (1) with transverse bias. $\langle \cos(2\pi y/L) \rangle$ vs g/U_0 for different values of D_0 . Vertical arrows are the relevant g_c values, Eq. (5). The flow parameters are $U_0 = 1$ and $L = 2\pi$, with $D_L = 1$. The dashed curve represents the analytical prediction of Eq. (3) for $D_0 \gg D_L$.

expected for $g = 0$, to narrowly peaked around the ascending laminar flow centered at $x = L/2$. For $Pe \gg 1$, this transition is very sharp and coincides with the D drop in Fig. 2 [21]. In contrast, for $Pe < 1$, $p(x)$ oscillates with maxima (minima) in correspondence with the ascending (descending) flows at $L/2$ ($L \bmod L$). The dynamical transition revealed by the g dependence of D and $p(x)$ is confirmed by the curves $\langle \cos(2\pi y/L) \rangle$ vs g , displayed in Fig. 3 for different values of D_0 . Numerical evidence points to the existence of one critical bias, g_c , for $Pe \gg 1$.

We consider first the regime of low Péclet numbers, where the LE for the longitudinal coordinate, $\dot{x} = U_0 \cos(2\pi y/L) \sin(2\pi x/L) + \xi_x(t)$, is analytically more tractable. For $D_0 \gg D_L$, the coordinates x and y are clearly decoupled, i.e., advection is negligible with respect to thermal diffusion. For $g \gtrsim U_0$, advection is negligible with respect to the bias as well, so that the average $\langle \cos(2\pi y/L) \rangle$ can be safely computed by approximating the particle's vertical pdf to $p(y) \propto \exp(-gy/D_0)$ with $0 \leq y \leq L/2$; hence

$$\langle \cos(2\pi y/L) \rangle = \coth(\pi/2X)/(1 + X^2), \quad (3)$$

with $X = D_0 U_0 / g D_L$, in good agreement with the simulation data of Fig. 3. Two relevant limits of Eq. (3) are 1 for $g/U_0 \gg D_0/D_L$ and $(2/\pi)(g/U_0)(D_L/D_0)$ for $1 \lesssim g/U_0 \ll D_0/D_L$. Therefore the process $x(t)$ boils down to a Brownian motion in a washboard potential of amplitude, $D_L \langle \cos(2\pi y/L) \rangle$, which depends on g and D_0 . This is a well-established problem [22]. Accordingly, the particle's pdf oscillates, as shown in Fig. 1(c), with minima (maxima) where the bias is parallel (antiparallel) to the descending (ascending) advection drag. The asymptotic diffusion constant D can also be computed analytically [Eq. (11.47) of Ref. [22]],

$$D/D_0 = I_0^{-2}[\langle \cos(2\pi y/L) \rangle D_L/D_0], \quad (4)$$

where $I_0[\dots]$ is the modified Bessel function.

We address now the more interesting regime of high Péclet numbers, where the decoupling argument leading to Eqs. (3) and (4) fails, because x and y are strongly coupled via $\psi(x, y)$. At $g = 0$, $\langle \cos(2\pi y/L) \rangle = 0$ for any value of D_0 , so that $p(x) = 1/L$ in both Figs. 1(b) and 1(c). On increasing g , the

FBLs get distorted until they finally break up. Indeed, the particle moves along the top branch of a FBL for a time of the order of a quarter of the circulation period, π/Ω_L , and during such a time interval, the bias pulls it downward by a length of about $g/4\Omega_L$. As such length grows comparable with the width of an unbiased FBL, $\delta = (D_0/\Omega_L)^{1/2}$, i.e., for $g > g_c$ with

$$g_c/U_0 = 4\sqrt{D_0/D_L}, \quad (5)$$

the FBL mechanism is suppressed. Upon dropping out of the top branch of a FBL, the particle is likely to get trapped into the bottom branch of the same FBL and then swept toward an ascending advective flow. This mechanism gives rise to the strongly peaked $p(x)$ curves of Fig. 1(b).

The existence of a critical dynamical transition for $g \sim g_c$ is confirmed by the observation that our qualitative estimate for g_c , Eq. (5), correctly locates the sharp $0 \rightarrow 1$ jump of the $\langle \cos(2\pi y/L) \rangle$ curves in Fig. 3. Moreover, for $g_c \lesssim g \ll U_0$, the rising branches of D versus D_0 in Fig. 2(b) collapse onto a universal curve (see inset) upon rescaling $D_0 \rightarrow D_0/g^2$, as suggested by Eq. (5). Finally, the abrupt profile change of the pdfs in Fig. 1(b) also occurs for $g \sim g_c$ [21].

The breakdown of the FBL mechanism implies that for $g > g_c$ the particle gets pinned down in the vicinity of the bottom array's edge, subjected to an effective washboard potential with amplitude $D_L \langle \cos(2\pi y/L) \rangle$. As a result, for sufficiently large values of g , Eq. (4) with $\langle \cos(2\pi y/L) \rangle \sim 1$ closely fits also the horizontal tails of the curves of Fig. 2(a) and the curves of Fig. 2(b) with $g \gg U_0$.

Longitudinal bias. If a transverse bias suppresses AED, what about a bias $\mathbf{F} = F(\cos\theta, \sin\theta)$ applied at a tunable angle θ with the array's axis? The FBL suppression mechanism introduced above for $Pe \gg 1$ applies under two conditions: (i) \mathbf{F} is oriented at an angle θ large enough to extract the particle out of the top (bottom) FBL branches, that is, $|\theta| > \theta_c$ with $\theta_c = g_c/U_0$, and (ii) $|F_y| > g_c$, with g_c given in Eq. (5). Under these conditions, the particle is pressed against the array's edges and is thus pinned to an effective washboard potential in the horizontal direction. Accordingly, for $|F_y| > g_c$ and $F \leq U_0$, the particle's mobility, $\mu = \langle \dot{x} \rangle / F_x$, and diffusion constant, D , in Fig. 4 drop to exponentially small values [22]. However, on increasing F , the longitudinal component of the bias, F_x , eventually wins over the pinning action of the edge advection flow. Depinning from a washboard potential of amplitude $D_L \langle \cos(2\pi y/L) \rangle \sim D_L$ occurs for $|F_x| \sim U_0$ [22] and is signaled by an excess-diffusion peak [23,24], marked by vertical arrows in Fig. 4(a). For vanishing and exceeding large values of F , μ approaches the expected horizontal asymptote, $\mu = 1$, whereas D tends to two distinct zero-bias limits, respectively, $\kappa\sqrt{D_L D_0}$ (as obvious being $Pe \gg 1$) and D_0 (like in the opposite $Pe \ll 1$ regime). Indeed, on increasing F much larger than U_0 , the effect of advection becomes negligible even for $Pe \gg 1$ (no high Péclet numbers AED, here!).

The curves D versus F at small bias angles hint to a totally different picture. Our simulation data show that for $\theta < \theta_c$, (i) the mobility is insensitive to advection, with $\mu = 1$ for any value of F [25], and (ii) the asymptotic constant D develops a broad peak for $F \lesssim U_0$, which can grow orders of magnitude larger than its asymptotic values for $F \rightarrow 0$

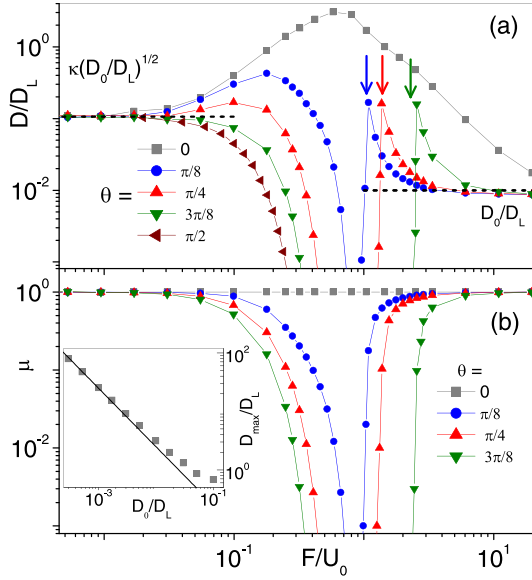


FIG. 4. Particle driven by a force \mathbf{F} at an angle θ with the array's axis: (a) D/D_L and (b) $\mu = \langle \dot{x} \rangle / F \cos \theta$ vs F/U_0 for different θ . Vertical arrows mark the predicted excess-diffusion peaks at the depinning threshold $|F_x| = U_0$; dashed lines denote the D asymptotes for $F \rightarrow 0$ and $F \rightarrow \infty$. Other simulation parameters are $L = 2\pi$, $U_0 = 1$, and $D_0/D_L = 0.01$. Inset: power-law fit of D_{\max}/D_L vs D_0/D_L for $\theta = 0$.

or $F \rightarrow \infty$. Such a huge diffusion enhancement results from the interplay of advection, applied (longitudinal) drive, and the array's geometry. We estimated the height of such an excess-diffusion peak, D_{\max} , as follows. By the time F comes close to U_0 , the FBLs around the individual convection rolls have long been gone; the particle can diffuse either along the central array's lane, with relatively low free diffusion constant D_0 , or along the array's edges, still subject to the advection drag with longitudinal velocity $\pm U_0$. The pinning action of the relevant washboard potential can be overcome even for $|F| \lesssim U_0$, since the particle can thermally diffuse across the array, i.e., transverse to its axis, with an average time of the order of $\tau_D = (L/2)^2/2D_0$. Moreover, the advection drag along the top and bottom array's edges are opposite in phase. Accordingly, for $F \sim U_0$ the particle's diffusion constant due to edge switching must be of the order of $D = \bar{U}_0^2 \tau_D / 2$, where

\bar{U}_0 is a suitable spatial average of the advection speed across the FBL (proportional to U_0); hence

$$D_{\max}/D_L \propto \text{Pe}.$$

Such a power-law divergence of D_{\max} for $D_0/D_L \rightarrow 0$ fits well the simulation data reported in the inset of Fig. 4(b). This is an interesting result when compared with the D_0 dependence of the height, D_{dep} , of the depinning excess-diffusion peaks centered at $|F_x| \sim U_0$ [marked by arrows in Fig. 4(a)], namely, $D_{\max}/D_0 \propto D_0^{-2}$ versus $D_{\text{dep}}/D_0 \propto D_0^{-2/3}$ [24]. The excess diffusion for $|\theta| < \theta_c$ is no boundary effect (under the same conditions it can be observed also in 2D convection arrays!) and, most remarkably, it can be made larger than the excess diffusion due to pinning at the array's boundaries, i.e., for $|\theta| > \theta_c$. The situation described in this section clearly differs, despite some apparent similarities, from the case of Brownian particles pumped through corrugated channels in the presence of a divergence-free force field [26].

Conclusions. The main conclusions of this study can be summarized saying that the FBL mechanism responsible for AED at high Péclet numbers is fluid mechanically rather weak. Applying a transverse bias with modulus above a critical value suffices to deactivate it, thus strongly suppressing particle diffusion. On the contrary, applying a longitudinal bias of modulus comparable with the advection speed causes a huge excess-diffusion peak. We have presented numerical evidence of both effects for the case of free-boundary convection arrays.

However, the overall picture presented above holds for no-slip arrays, as well. Simulation data for a simple example are presented in the Supplemental Material [21]. In the presence of a transverse bias g , the breakdown of the FBL mechanism is still detectable, though not as sharp as in free-slip arrays. On the other hand, the particle's diffusion constant, D , still drops sharply with increasing g , except for $g \gtrsim g_c$ it now rises back toward its free value, D_0 . Such a *reentrant diffusivity* happens because a particle sliding against the edges of a no-slip array is advection free, and its diffusion is controlled by the sole thermal fluctuations.

Acknowledgments. Y.L. is supported by the NSF China under Grants No. 11875201 and No. 11935010. P.K.G. is supported by a SERB Start-up Research Grant (Young Scientist) No. YSS/2014/000853 and the UGC-BSR Start-Up Grant No. F. 30-92/2015. T.D. thanks UGC, New Delhi, India, for support through a Senior Research Fellowship.

[1] B. J. Kirby, *Micro- and Nanoscale Fluid Mechanics: Transport in Microfluidic Devices* (Cambridge University Press, Cambridge, England, 2010).
 [2] P. Tabeling, Two-dimensional turbulence: A physicist approach, *Phys. Rep.* **362**, 1 (2002).
 [3] X. Yang, C. Liu, Y. Li, F. Marchesoni, P. Hänggi, and H. P. Zhang, Hydrodynamic and entropic effects on colloidal diffusion in corrugated channels, *Proc. Natl. Acad. Sci. USA* **114**, 9564 (2017).
 [4] S. Chandrasekhar, *Hydrodynamic and Hydromagnetic Stability* (Oxford University Press, New York, 1967).

[5] S. Childress, Alpha-effect in flux ropes and sheets, *Phys. Earth Planet. Int.* **20**, 172 (1979).
 [6] *Topological Aspects of the Dynamics of Fluids and Plasmas*, edited by H. K. Moffatt, G. M. Zaslavsky, P. Comte, and M. Tabor (Springer, Netherlands, 1992).
 [7] M. N. Rosenbluth, H. L. Berk, I. Doxas, and W. Horton, Effective diffusion in laminar convective flows, *Phys. Fluids* **30**, 2636 (1987).
 [8] A. M. Soward, Fast dynamo action in a steady flow, *J. Fluid Mech.* **180**, 267 (1987).

- [9] B. I. Shraiman, Diffusive transport in a Rayleigh-Bénard convection cell, *Phys. Rev. A* **36**, 261 (1987).
- [10] W. Young, A. Pumir, and Y. Pomeau, Anomalous diffusion of tracer in convection rolls, *Phys. Fluids* **1**, 462 (1989).
- [11] Q. Yin, Y. Li, F. Marchesoni, T. Debnath, and P. K. Ghosh, Exit times of a Brownian particle out of a convection roll, *Phys. Fluids* **32**, 092010 (2020).
- [12] A. Crisanti and A. Vulpiani, On the effects of noise and drift on diffusion in fluids, *J. Stat. Phys.* **70**, 197 (1993).
- [13] P. E. Kloeden and E. Platen, *Numerical Solution of Stochastic Differential Equations* (Springer, Berlin, 1992).
- [14] C. Gardiner, *Stochastic Methods: A Handbook for the Natural and Social Sciences* (Springer, Berlin, 2009).
- [15] Y. Li, L. Li, F. Marchesoni, D. Debnath, and P. K. Ghosh, Active diffusion in convection rolls, *Phys. Rev. Res.* **2**, 013250 (2020).
- [16] T. H. Solomon and J. P. Gollub, Passive transport in steady Rayleigh-Bénard convection, *Phys. Fluids* **31**, 1372 (1988).
- [17] T. H. Solomon and I. Mezić, Uniform resonant chaotic mixing in fluid flows, *Nature (London)* **425**, 376 (2003).
- [18] Y.-N. Young and M. J. Shelley, Stretch-Coil Transition and Transport of Fibers in Cellular Flows, *Phys. Rev. Lett.* **99**, 058303 (2007).
- [19] H. Manikantan and D. Saintillan, Subdiffusive transport of fluctuating elastic filaments in cellular flows, *Phys. Fluids* **25**, 073603 (2013).
- [20] C. Torney and Z. Neufeld, Transport and Aggregation of Self-Propelled Particles in Fluid Flows, *Phys. Rev. Lett.* **99**, 078101 (2007).
- [21] See Supplemental Material at <http://link.aps.org/supplemental/10.1103/PhysRevE.103.L030106> for additional simulation results.
- [22] H. Risken, *The Fokker-Planck Equation* (Springer, Berlin, 1984), Chap. 11.
- [23] G. Costantini and F. Marchesoni, Threshold diffusion in a tilted washboard potential, *Europhys. Lett.* **48**, 491 (1999).
- [24] P. Reimann, C. Van den Broeck, H. Linke, P. Hänggi, J. M. Rubi, and A. Pérez-Madrid, Giant Acceleration of Free Diffusion by use of Tilted Periodic Potentials, *Phys. Rev. Lett.* **87**, 010602 (2001).
- [25] A. Sarracino, F. Cecconi, A. Puglisi, and A. Vulpiani, Nonlinear Response of Inertial Tracers in Steady Laminar Flows: Differential and Absolute Negative Mobility, *Phys. Rev. Lett.* **117**, 174501 (2016).
- [26] S. Martens, A. Straube, G. Schmid, L. Schimansky-Geier, and P. Hänggi, Hydrodynamically Enforced Entropic Trapping of Brownian Particles, *Phys. Rev. Lett.* **110**, 010601 (2013).